ACCSCIENCE PUBLISHING

Tumor Discovery

ORIGINAL RESEARCH ARTICLE

The role of pyroptosis-related genes in breast cancer progression

Shanshan Wang[1†], Dashuang Yang[2†], Jiaqian Mo[1], Moxian Chen[3], and Rongxin Zhang[1*]

[1]Department of Life Sciences and Biopharmaceutics, Guang Dong Pharmaceutical University, Guangzhou, Guangdong, China

[2]Guangdong-Hong Kong-Macau Institute of CNS Regeneration, Jinan University, Guangzhou, Guangdong, China

[3]State Key Laboratory of Tree Genetics and Breeding, Co-Innovation Center for Sustainable Forestry in Southern China and College of Life Sciences, Nanjing Forestry University, Nanjing, Jiangsu, China

Abstract

Breast cancer (BC) is one of the most common malignant cancers affecting females worldwide. Pyroptosis, a form of programmed cell death associated with inflammation and triggered by pro-inflammatory signals, is not well understood in the context of BC. This study aimed to investigate the role of pyroptosis in BC patients. Paired tumor and adjacent normal tissue samples were obtained from The Cancer Genome Atlas. Using a least absolute shrinkage and selection operator Cox analysis, we identified 15 prognostic genes associated with BC. Among these, fibrinogen C domain-containing 1, calcium voltage-gated channel subunit alpha1 H, heat shock protein family B (small) member 8, and peroxidasin-like (*PXDNL*) were classified as high-risk genes in BC. In contrast, the remaining 11 genes, such as proteasome activator subunit 2 and *DIRAS* (DIRAS family GTPase 3), were low-risk genes. Kyoto Encyclopedia of Genes and Genomes and Gene ontology analyses revealed that immune-related genes were enriched but showed reduced immunological status in the high-risk group, indicating that pro-inflammatory factors and immune antigens were produced during cell death. Consequently, targeting immune antigens with new immunosuppressants may offer a novel approach to treating BC. Moreover, the expression levels of the prognostic genes *PXDNL*, armadillo-like helical domain-containing 1 (*ARMH1*), *APOBEC3D*, and *APOBEC3F* in BC cell lines were assessed using quantitative polymerase chain reaction and western blotting. *PXDNL* and *ARMH1* exhibited high levels of expression in BC, suggesting they could be potential therapeutic targets.

Keywords: Breast cancer; Pyroptosis; Inflammation; Prognostic genes; The cancer genome atlas

***Corresponding author:**
Rong-Xin Zhang
(rxzhang@gdpu.edu.cn)

Citation: Wang S, Yang D, Mo J, Chen M, Zhang R. The role of pyroptosis-related genes in breast cancer progression. *Tumor Discov.* 2024;3(3):3469.
doi: 10.36922/td.3469

Received: April 23, 2024

Accepted: August 19, 2024

Published Online: September 24, 2024

Copyright: © 2024 Author(s). This is an Open-Access article distributed under the terms of the Creative Commons Attribution License, permitting distribution, and reproduction in any medium, provided the original work is properly cited.

Publisher's Note: AccScience Publishing remains neutral with regard to jurisdictional claims in published maps and institutional affiliations.

1. Introduction

Breast cancer (BC) is one of the most common malignant cancers affecting women worldwide and is the second cause of cancer-related death among women, with high morbidity and mortality rates.[1,2] By the end of 2020, BC had been detected in 7.8 million

women over the previous 5 years, making it the world's most common malignancy. Although BC can affect women of any age after puberty, its incidence is higher in older age.[3] Unfortunately, the incidence of BC has been increasing annually in many countries and regions.[4] In response to this, the World Health Organization's Global BC Initiative aims to reduce global BC mortality by 2.5% annually between 2020 and 2040, with the goal of preventing 2,500,000 BC deaths worldwide. If successful, this effort could prevent 25% of BC deaths by 2030 and 40% by 2040 among women under 70. Achieving these objectives will require three key components: rapid diagnosis, thorough BC care, and health promotion for early detection. However, there is an urgent need for new tools for early diagnosis and prognosis to achieve these goals.[3]

Studies on pyroptosis[5] have revealed its significant role in tumor mechanisms. This understanding helps provide new ideas for a wide range of malignant cancers, including stomach, lung, and BCs. Pyroptosis, also referred to as inflammatory pyroptosis, is considered to be a new kind of programmed cell death related to gasdermin pores in the plasma membrane.[6,7] The main characteristics of pyroptosis include unique DNA damage, preservation of nuclear integrity, and the rapid formation of membrane pores with diameters of 10 – 15 nm. These pores lead to the gradual loss of cell ions, causing cell edema, membrane rupture, and the release of cellular contents and pro-inflammatory mediators. The process is faster and more intense than apoptosis.[8] The main executor of pyroptosis is the gasdermin family, including pejvakin (PJVK or DFNB59) and gasdermin-A to gasdermin-E. Inflammasomes, which are composed of oligomerized pattern recognition receptors (PRRs), procaspase-1, and the adaptor apoptosis-associated speck-like protein (ASC), play a crucial role in this process. In addition, ASC contains an N-terminal pyrin domain and C-terminal caspase recruitment domain (CARD) to recruit NOD-like proteins (NLRs), or, if it lacks the absent in melanoma 2-like receptor family and pro-caspase-1 for assembling the inflammasome, it activates caspase-1. According to the detection of damage signals by the cytoplasmic protein sensor, the mechanism of pyroptosis can be classified into two main pathways, the classic caspase-1-dependent pathway and the non-classic non-caspase-1-dependent pathway. In the classic caspase-1-dependent pathway, inflammasomes cleave the executive protein GSDMD by activating caspase-1, and the resulting GSDMD-N punches holes in the cell membrane to form non-selective membrane channels, disrupting the ion balance across the cell membrane. This disruption leads to cell swelling and lysis, and eventually, cell death. Moreover, pro-interleukin-1β and pro-Interleukin-18 are segmented by activated caspase-1, releasing these cytokines outside the cell to further mediate pyroptosis. The non-classic caspase-4/5/11 directly binds with lipopolysaccharide; then, through dimerization-induced autoproteolysis, these caspases are activated, which, in turn, leads to pyroptosis. In addition to the above-mentioned pyroptosis pathways, there are caspase-3/8-mediated pathways and serine protease-mediated pathways[9] (Figure 1). At present, pyroptosis has been widely studied as a new means of treating cancer, which suggests a new foundation for the prevention and treatment of this disease.

However, although pyroptosis is involved in the physiological and pathological processes of BC,[10] its role in BC has not been extensively studied. In this study, we aimed to investigate the roles of pyroptosis in patients with BC, which may provide a new tool for early diagnosis and prognosis in BC. A method of BC prognosis was established based on the degree of pyroptosis. First, the BC clinical data and the RNA sequencing were acquired from The Cancer Genome Atlas (TCGA) database. Thirty-nine differential genes were obtained by analyzing the differences in cell-death-related genes. After identifying these different genes by means of protein-protein interaction (PPI) and correlation network analyses, a pyroptosis-related gene prognostic model was developed and validated. Finally, Gene ontology (GO), Kyoto Encyclopedia of Genes and Genomes (KEGG), and ssGESA were utilized for functional and immunity analysis (Figure 2).

2. Methods

2.1. Data acquisition

In this study, the RNA sequencing and clinical documents of BC were obtained from the TCGA website on August 19, 2021. There were 112 cases in the normal group and 1106 cases in the tumor group (https://portal.gdc.cancer.gov/).

2.2. Identification of differentially expressed pyroptosis-related genes

Fifty-two pyroptosis-related genes were extracted to determine the differential genes between the normal group and the tumor group. The "limma" package within the R package was used to distinguish the differential genes with $P < 0.05$, which was marked as $^{*}P < 0.05$, $^{**}P < 0.01$, and $^{***}P < 0.001$, respectively (Figure 3A). Utilizing the search tool for the retrieval of interacting genes, the protein interaction network was obtained (Figure 3B). In addition, a correlation network was obtained using the "igraph" and "reshape2" packets (Figure 3C).

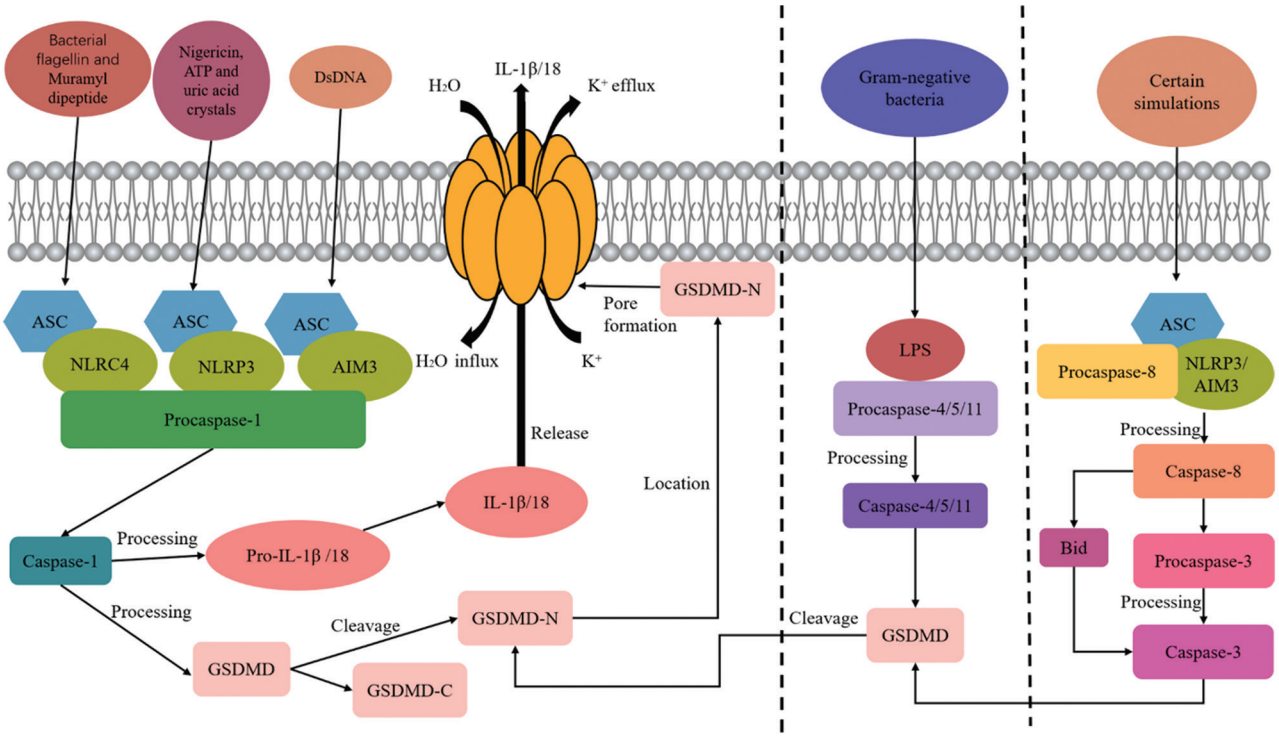


Figure 1. Pyroptosis pathway. First of all, inflammasomes are composed of oligomerized PRRs, procaspase-1, and the adaptor apoptosis-associated speck-like protein (ASC). Besides, ASC contains N-terminal pyrin domain and C-terminal caspase recruitment domain to recruit NOD-like proteins or absent in melanoma 2-like receptor family and pro-caspase-1 to assemble inflammasome, then activates caspase-1. According to the recognition of damage signals by cytoplasmic protein sensors, the mechanism of pyroptosis can be separated into a classical caspase-1-dependent pathway and a non-classical non-caspase-1-dependent pathway. The classical caspase-1-dependent pathway is that inflammasomes cut the executive protein GSDMD by activating caspase-1, and the resulting GSDMD-N punches holes in the cell membrane to form non-selective membrane channels, resulting in the destruction of ion concentration balance on both sides of the cell membrane, swelling and lysis of cells, and eventually death. Moreover, pro-interleukin-1β and pro-IL-18 can be segmented by activated caspase-1, and the resultant IL-1β and IL-18 are released outside of the cell, which mediates pyroptosis. Caspase-4/5/11 directly binds with lipopolysaccharide (LPS), and then, through dimerization-induced autoproteolysis, these caspases get activated, which, in turn, leads to pyroptosis. In addition to the above-mentioned pyroptosis pathways, there are caspase-3/8-mediated pathways and serine protease-mediated pathways.

2.3. Establishment and validation of pyroptosis-related gene prognostic model

According to the expression of the pyroptosis genes, the samples were clustered and typed. Then, the survival analysis of patients with different types was performed to observe whether there were differences between the two types of patients. In addition, 15 prognostic genes were obtained by further screening the data downloaded from the TCGA. The following formula was used to calculate the risk score (Equation I):

$$Risk\ score = \sum_{i}^{15} X_i \times Y_i \qquad \text{I)}$$

Where X is the coefficient and Y is the gene expression level. Thus, the patients were classified as high-risk and low-risk groups, and the prognostic model of the TCGA cohort was obtained by using the risk score formula. To further verify the accuracy of the TCGA data prognosis model, principal component analysis (PCA), a receiver operating characteristic (ROC) curve, and other methods were employed.

2.4. Independent TCGA prognostic analysis of the risk score

This model utilized an independent prognostic factor and other clinical traits and was verified by means of univariate and multivariate Cox regression analysis.

2.5. Functional enrichment analysis

Based on their median risk scores, patients with BC in the TCGA cohort were divided into two different subgroups. The differential genes between the high- and low-risk groups were sifted based on the specific criteria ($P < 0.05$; $Q < 0.05$). Based on these differential genes, the "clusterProfiler" package was used for GO and KEGG analysis. The "gsva" package was applied to conduct a

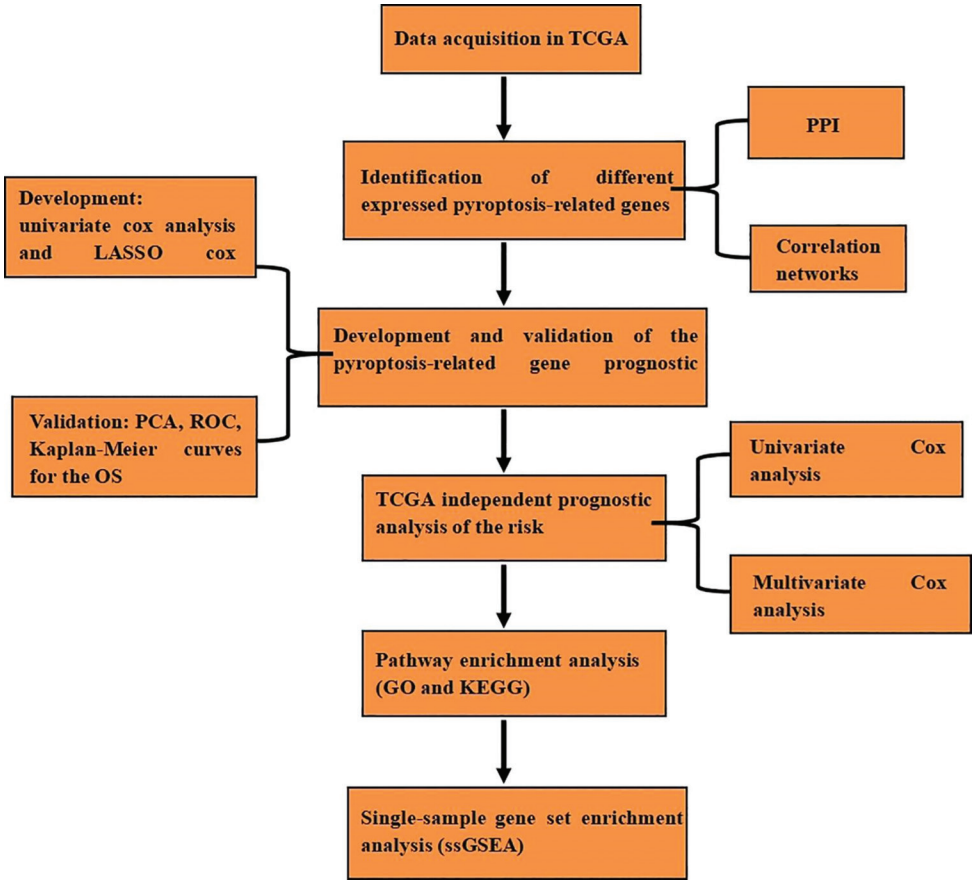


Figure 2. Workflow. The method of breast cancer (BC) prognosis was established through the degree of pyroptosis. First, the BC clinical data and the RNA sequencing were acquired from the TCGA database. Thirty-nine differential genes were obtained through the differences of cell-death-related genes analyzed. After identifying these different genes by PPI analysis and correlation network, a pyroptosis-related gene prognostic model was developed and validated. Finally, GO, KEGG, and ssGESA were utilized for functional and immunity analysis.
Abbreviations: GO: Gene ontology; KEGG: Kyoto Encyclopedia of Genes and Genomes; LASSO: Least absolute shrinkage and selection operator; OS: Overall survival; PCA: Principal component analysis; PPI: Protein-protein interaction; ROC: Receiver operating characteristic; TCGA: The Cancer Genome Atlas.

single-sample gene set enrichment analysis (ssGSEA) to determine the immune cell infiltration score and assess the activity of the immune-related pathways.

2.6. Cell lines

Normal human mammary epithelial cells (MCF10 A) and BC cell lines (MDA-MB-231, MDA-MB-468, BT549, and MCF-7) were purchased from the American Type Culture Collection, China. MCF10 A cells were cultured in MCF10 A-specialized media (CM-0525, Pricella, China), while all other cell lines were cultured in DMEM (Meilunbio, MA0212) with 10% Fetal Bovine Serum (086 – 150, WISENT, China), and a 1% Penicillin-Streptomycin Solution (100×) (P1400, Solarbio, China). All cells were incubated at 37°C and 5% CO_2 in an incubator.

2.7. RNA extraction and quantitative polymerase chain reaction (qPCR)

Total RNAs were extracted from cells according to protocols provided by the manufacturer using a TRIzol reagent (Takara, China), and cDNA synthesis was performed using an RT6 cDNA synthesis kit (Tsingke, China) and following the protocols. In addition, in accordance with instructions, qPCR was carried out using the ChamQ SYBR qPCR Master Mix (Vazyme, China). The primers are listed in Table 1. The $2^{-\Delta\Delta Ct}$ values were determined, and data were analyzed using GraphPad Prism 8. *P*-values: $^{*}P < 0.05$; $^{**}P < 0.01$; $^{***}P < 0.001$.

2.8. Western blotting

The total cell proteins were extracted using RIPA lysis buffer (Applygen, China) supplemented with 1%

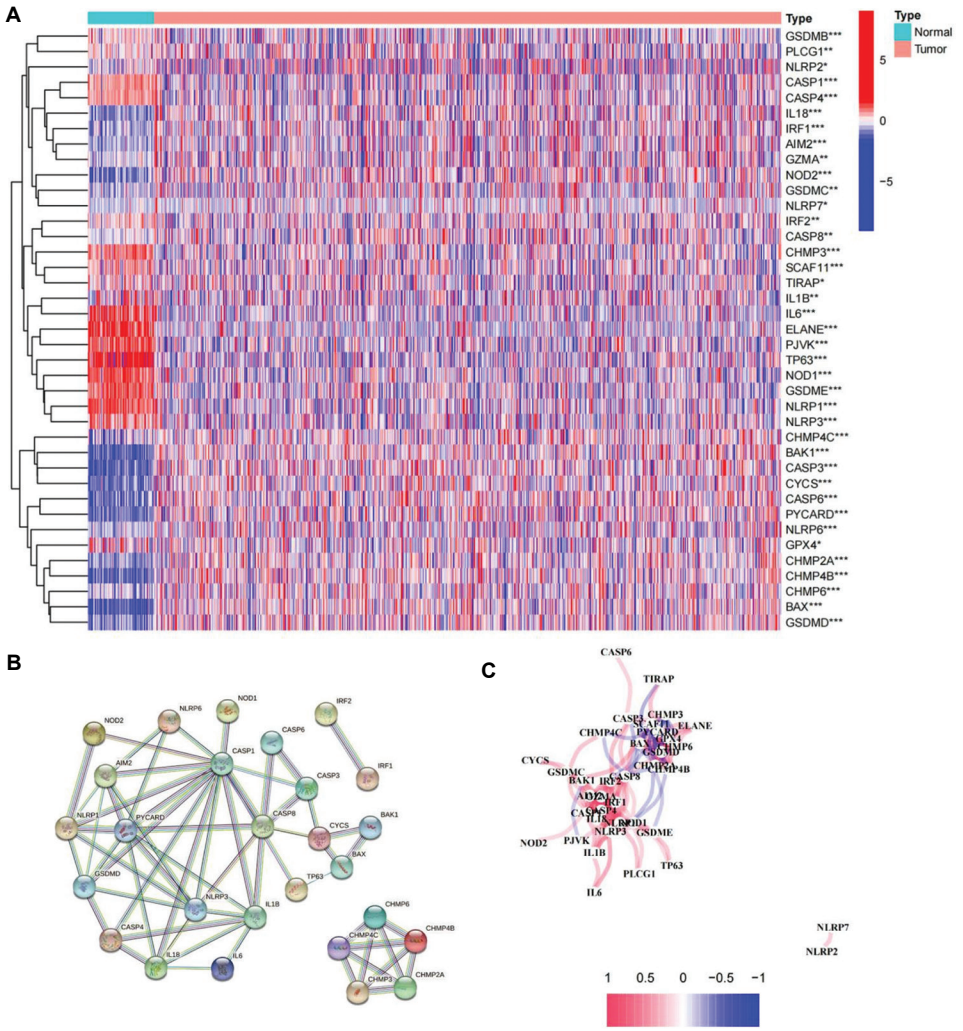


Figure 3. The expression level of the 39 pyroptosis-related genes and their interactions. (A) Heatmap (red: high expression level; blue: low expression level) of pyroptosis-related genes in normal (N, pale blue) and tumor tissues (T, red). (B) Protein-protein interaction network illustrating pyroptosis-related gene interactions (interaction score = 0.9). (C) The pyroptosis-related gene correlation network (blue line: Negative correlation; red line: Positive correlation). The strength of the relevance is reflected in the color depth.
Notes: P-values: *P < **0**.05; **P < 0.01; ***P < 0.001.

protein phosphatase inhibitor (Solarbio, China) and 1% phosphatase inhibitor (Beyotime, China) and were analyzed by means of western blotting using the following antibodies: peroxidasin-like (anti-PXDNL) (YM0524, ImmunoWay Biotechnology, America), armadillo-like helical domain-containing 1 (anti-ARMH1) (TA334858, Origene, China), anti-GAPDH (52902, Signalway Antibody, China), and anti-APOBEC3D/APOBEC3F (PA5 – 101777, Invitrogen, China) were used. Stripping buffer (CW0056M [500 mL], CWBIO, China) was used to remove primary and secondary antibodies from the imprinted membrane, enabling multiple antibody detection on the same membrane. Protein bands were quantified with ImageJ software. Finally, the absolute expressions were determined, and the data were analyzed using GraphPad Prism 8. Statistical significance was assessed as follows: *P < 0.05; **P < 0.01; ***P < 0.001.

2.9. Statistical analysis

The data from the qPCR are expressed as the relative expression in terms of $2^{-\Delta\Delta Ct}$, while the data from the western blotting are expressed as the absolute expression. A Student's t-test was used to compare continuous variables. A P < 0.05 was considered statistically significant. Data were analyzed using GraphPad Prism 8.

Table 1. Primers used in qPCR

Oligo name	Sequence (5' to 3')
ARMH1	Forward: GGC AGC AAT TAG CAG GCT CTT
	Reverse: GAA CTT GTC GAG GAT GTG ACT C
PXDNL	Forward: GAG ACC TTC TGA GAT TAG AGC GA
	Reverse: GCG TTG GAA TCC AGA CGC A
APOBEC3D	Forward: CTT TCG AGG CCC GGT ACT AC
	Reverse: GTG ATC TGG AAG CGC CTG TTA
APOBEC3F	Forward: CTT CAG AAA CAC AGT GGA GCG AAT G
	Reverse: GTA GCA CAG CCA GAC GGT ATT CC
GAPDH	Forward: CAT GAG AAG TAT GAC AAC AGC CT
	Reverse: AGT CCT TCC ACG ATA CCA AAG T

Abbreviations: qPCR: quantitative polymerase chain reaction. *PXDNL*: Peroxidasin-like; *ARMH1*: Armadillo-like helical domain-containing 1.

3. Results

3.1. Confirmation of differential genes between tumor and normal tissues

We downloaded mRNA sequencing data from the TCGA for the normal group (n = 112) and the tumor group (n = 1066). A total of 52 different pyroptosis-related genes were identified, and 39 differential genes were obtained ($P < 0.05$). There were 17 down-regulated genes, including *IL6* and *TP63*, and 22 up-regulated genes, including *CASP8* and *CHMP6* (Figure 3A). To analyze the interaction of these pyroptosis-related genes, PPI analysis was utilized (Figure 3B). The minimum required interaction score for the PPI analysis was 0.9, indicating the highest confidence. The hub genes identified were *CAPS1*, *PYCARD*, *CASP8*, *NLRP3*, and *IL1B*. A correlation threshold of 0.2 was applied to the correlation network (Figure 3C), revealing a significant relationship among these genes.

3.2. Tumor classification based on differential genes

We analyzed a total of 654 BC patients (stages II, IV, and V) from the TCGA cohort to investigate the relationship between BC subtypes and the expression of 39 differential pyroptosis-related genes using consensus clustering analysis. The analysis revealed that, as the number of clustering variables (k) increased from two to nine, the intragroup correlations were highest, and intergroup correlations were lowest at k = 2. This suggests that the 654 BC patients can be effectively categorized into two groups (Figure 4A). Gene expression profiles and clinical characteristics, including survival status (alive or dead) and survival time (≤65 years or >65 years), were displayed on a heatmap, but no significant clinical features were found between the two groups (Figure 4B). In addition, we found that there were significant differences in overall survival (OS) times between the two clusters ($P < 0.001$; Figure 4C).

3.3. Establishment and validation of pyroptosis-related gene prognostic model

We compared the expression of 1,231 genes in 627 BC patients to identify prognosis-related genes using univariate Cox regression analysis. Fifty-five genes were selected for further analysis ($P < 0.01$; Figure 5A). Among these, five high-risk genes were fibrinogen C domain-containing 1 (*FIBCD1*), calcium voltage-gated channel subunit alpha1 H (*CACNA1H*), *FAM234B*, heat shock protein family B (small) member 8 (*HSPB8*), and *PXDNL*, while the remaining 50 genes were low-risk genes. Based on the optimal value, 15 gene signatures were generated using the least absolute shrinkage and selection operator Cox regression analysis (Figure 5B and C).

The following formula was used to determine the risk score (Equation II):

$$\begin{aligned} Risk\ Score = {} & (0.125)\times e^{FIBCD1} + (0.122)e^{PXDNL} \\ & + (0.099)\times e^{HSPE8} + (0.019)e^{CACNA1H} + (-0.008)\times e^{RGS1} \\ & + (-0.012)\times e^{MMP7} + (-0.029)\times e^{APOBEC3D} \\ & + (-0.047)\times e^{PSME2} + (-0.058)\times e^{APOBEC3F} + (-0.073) \\ & \times e^{KLHDC7B} + (-0.082)\times e^{RAC2} + (-0.100)\times e^{MATK} + (-0.165) \\ & \times e^{DEF6} + (-0.250)\times e^{APMH1} + (-0.281)\times e^{DIRAS3} \end{aligned} \quad \text{(II)}$$

The risk score formula's median score was used to categorize the 627 patients with BC into high- and low-risk categories (Figure 5D). Through PCA and t-distributed stochastic neighbor embedding, the individuals were clearly divided into two different clusters (Figure 5E and F: blue dot – low-risk group; red dot – high-risk group). The OS time of the high- and low-risk subgroups differed considerably ($P < 0.001$, Figure 5G and H). In addition, the area under the curve of the ROC was 0.650 for 1 year, 0.792 for 2 years, and 0.696 for 3 years of survival, which indicated that there was a certain degree of credibility in the prediction of patients' survival times (Figure 5I). In conclusion, the reliability of the pyroptosis-related gene prognostic model was established and validated.

3.4. Independent prognostic value of the risk model for the TCGA cohort

The risk score derived from the TCGA cohort was used to predict low survival, serving as a completely autonomous prognostic factor, according to the univariate Cox regression analysis (hazard ratio [HR] = 4.504; confidence interval [CI]: 2.855 – 7.108; Figure 6A). The

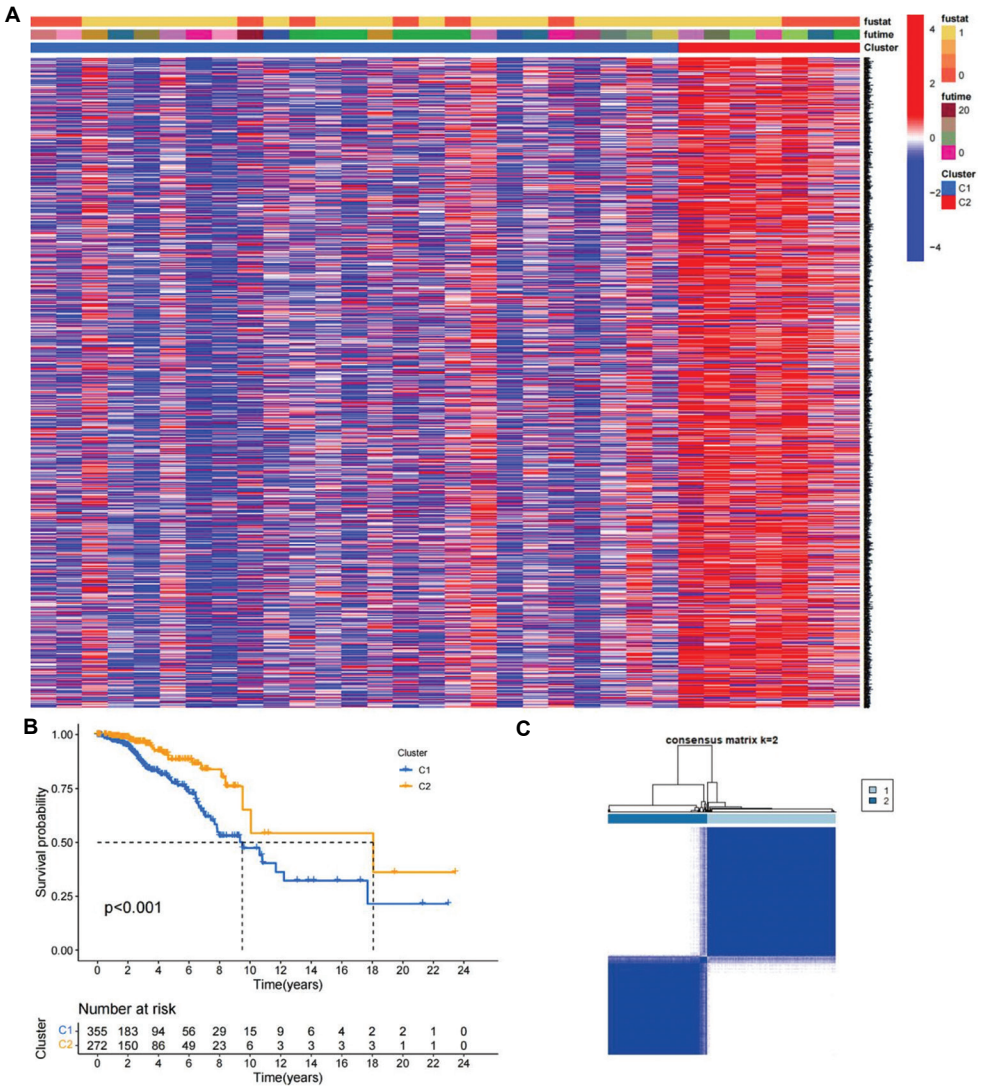


Figure 4. Differential genes related to pyroptosis are used for tumor classification. (A) Heatmap depicting the two clusters grouped by the differential genes. (B) Kaplan-Meier overall survival (OS) curves for the two different clusters. (C) The consensus clustering matrix (k = 2) was used to separate 654 patients with breast cancer into two different groups.

multivariate Cox regression analysis showed that the risk score for the patients with BC in the TCGA cohort was also an independent prognostic predictor after correcting for other confounding factors (HR = 4.353, CI: 2.638 − 7.183, Figure 6B). To further analyze the connections between clinicopathologic features and risk groups, a heatmap was constructed for the TCGA cohort, which revealed that the age, survival status, and gender of the patients were diversely distributed across the two subgroups ($P < 0.01$, Figure 6C).

3.5. Functional analyses based on the risk model

To investigate the variations in gene functions and pathways amongst the subgroups separated by the risk model, the differential genes were extracted using the "limma" package, and false discovery rate < 0.05 and | log2FC | ≥ 1 were applied. The TCGA cohort yielded a total of 100 different genes between the low- and high-risk categories. Among these, in the high-risk group, 88 genes were down-regulated, and the remaining 12 genes were up-regulated. On this basis, GO and KEGG analyses were performed ($P < 0.05$). The results of the GO analysis (Figure 7) showed that the differential genes were primarily correlated with the leukocyte cell-cell adhesion and cell chemotaxis in the biological process, the plasma membrane's outer layer in the cellular component, and antigen binding in the molecular function. The KEGG pathway is mainly involved in cytokine-cytokine receptor interactions, human T-cell leukemia virus 1

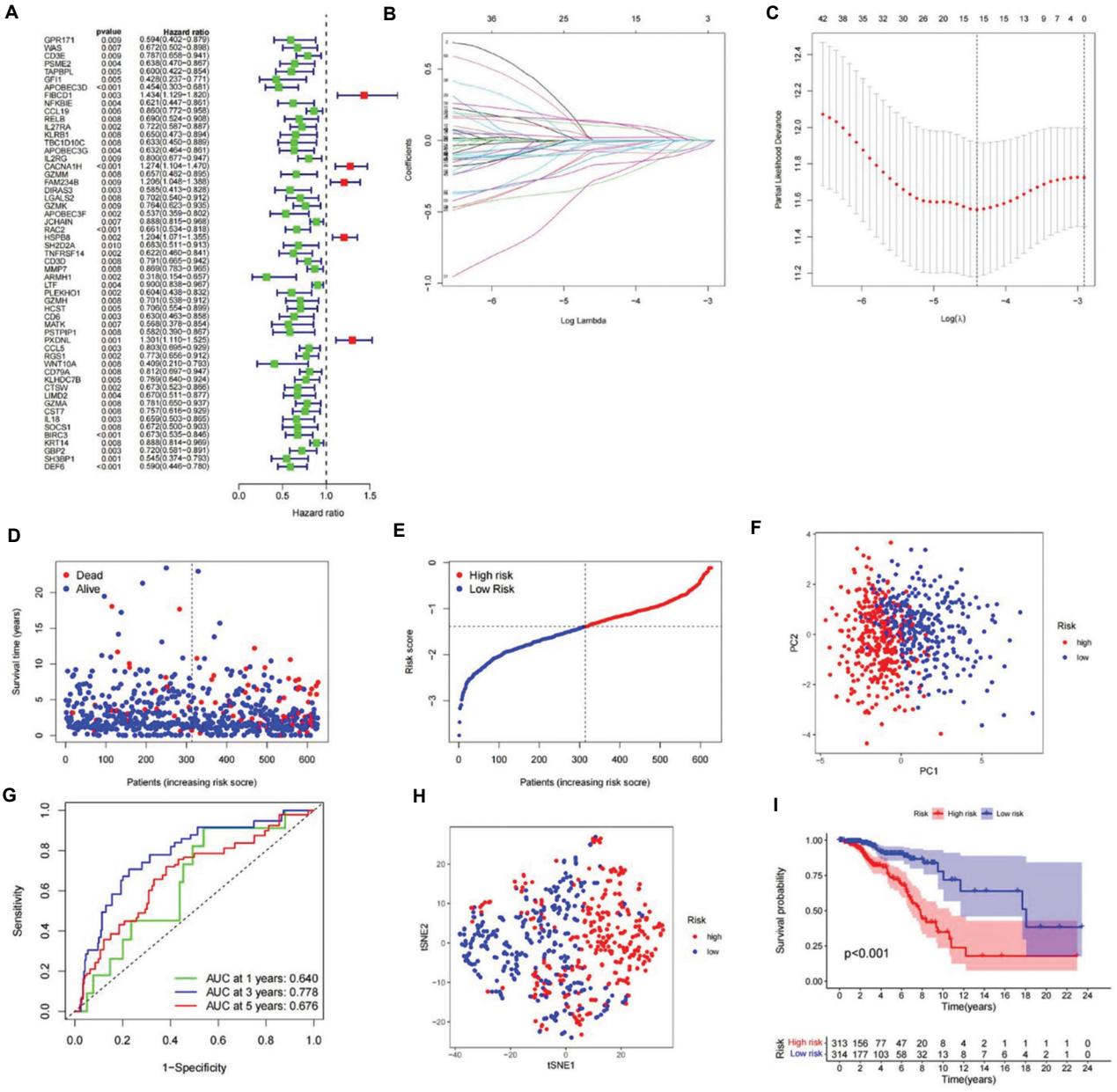


Figure 5. The Cancer Genome Atlas cohort was used to create a risk signature. (A) Overall survival (OS) univariate Cox regression analysis for every gene associated with prognosis, with $P < 0.01$. (B) Least absolute shrinkage and selection operator (LASSO) regression analysis of these 15 individual OS-related prognosis-related genes. (C) Cross-validation is used in LASSO regression to optimize parameter selection. (D) Patient distribution depends on the risk score. (E) Principal component analysis plot calculated based on the breast cancer risk score. (F) A t-distributed stochastic neighbor embedding plot was calculated based on the breast cancer risk score. (G) Kaplan-Meier curves for the OS of low and high-risk patients. (H) Every patient's transformation of survival (low-risk population: on the left side of the dotted line; high-risk population: on the right side of the dotted line). (I) Receiver operating characteristic curves were used to demonstrate the risk score's predictive efficacy.

infection, *Staphylococcus aureus* infection, and Th17 cell differentiation (Figure 8).

Using ssGSEA, we compared the high- and low-risk groups in the TCGA cohort by looking at the enrichment scores of 16 different immune cell types and the activity of 13 different types of immune-related pathways. When the immune cells were analyzed, we discovered that the level of infiltration in the high-risk group was lower than that in the low-risk group, particularly for B cells, CD8+ T cells, natural killer cells, T helper (Th) cells (Thf, Th1,

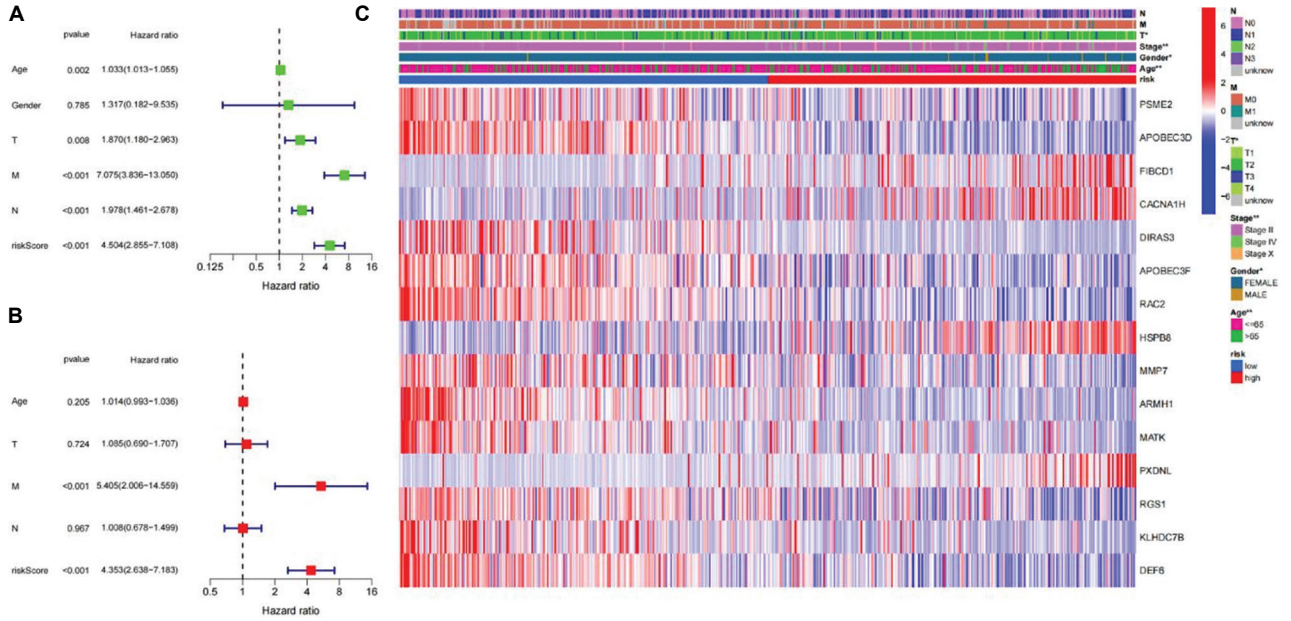


Figure 6. Cox regression analysis for the risk score, both univariate and multivariate. (A) The Cancer Genome Atlas (TCGA) cohort's univariate analysis. (B) TCGA cohort's multivariate analysis. (C) Heatmap of the associations between clinicopathologic characteristics and risk groups (*$P < 0.05$, **$P < 0.01$, blue: low expression, red: high expression).

and Th2 cells), and tumor-infiltrating lymphocytes. All the *P*-values were below 0.001, with the exception of those for mast cells (Figure 9A). In the analysis of immune pathways, we discovered that, in the high-risk group, the activity of 13 immune pathways was significantly lower than that in the low-risk group, and all the *P*-values were below 0.001 (Figure 9B), which indicated a significant difference in this model.

4. Discussion

Among the 15 gene signatures identified using the optimal λ value, we concluded that *FIBCD1*, *CACNA1H*, *HSPB8*, and *PXDNL* were high-risk genes involved in BC pyroptosis. Meanwhile, the other 11 genes, namely, DIRAS family GTPase 3 (*DIRAS3*), *APOBEC3F*, *RAC2*, matrix metallopeptidase 7 (*MMP7*), proteasome activator subunit 2 (*PSME2*), *ARMH1*, megakaryocyte-associated tyrosine kinase (*MATK*), regulator of G protein signaling 1 (*RGS1*), *KLHDC7B*, guanine nucleotide exchange factor (*DEF6*), and *APOBEC3D*, were low-risk genes. Notably, *FIBCD1*, identified as a "potential" pyroptosis-related gene, was related to inflammation.

FIBCD1, a recognition receptor, can recognize complex polysaccharides and regulate inflammatory responses by inhibiting inflammatory mediators and mucinous proteins. In addition, it has already been reported to be significantly elevated in various malignant cancers, including hepatocellular carcinoma and BC.[11,12] In this study, *FIBCD1* was up-regulated, suggesting a need for further research to discover its role in mediating BC cells. Several genes associated with invasion and metastasis — *CACNA1H*, *DIRAS3*, *RAC2*, *MMP7*, *MATK*, and *DEF6* — may contribute to the acceleration of BC cell progression.

First, the CACNA1H is a form of voltage-sensitive calcium channel that generates a T-type calcium current by increasing intracellular calcium influx, resulting in the activation of p38MAPK. Current research indicates that using a specific frequency of 27.12 MHz can significantly inhibit the metastatic growth in the brain caused by the activation of CACNA1H in BC.[13-15] Second, DIRAS3 is a member of the Ras superfamily, a tumor suppressor inhibiting the signal transduction, growth, and movement of cancer cells through Phosphatidylinositol 3-kinase/AKT, JAK/STAT, and RAS/MAPK.[16] Third, Rac family small GTPase 2 (RAC2) is a member of the Ras superfamily of small guanosine triphosphate-metabolizing proteins and could be crucial in controlling the actin cytoskeleton during BC development.[17] To further improve prognosis, a joint study of BC and immune pathways may be carried out in the future. Fourth, MMP7 is a member of the matrix metalloproteinase (MMP) peptidase M10 family and shows increased expression in a variety of human cancers. MMP7 is an independent prognostic factor for BC metastasis through suppressing the recruitment of CD4+/CD8+ tumor-infiltrating lymphocytes or the expression of C-X-C

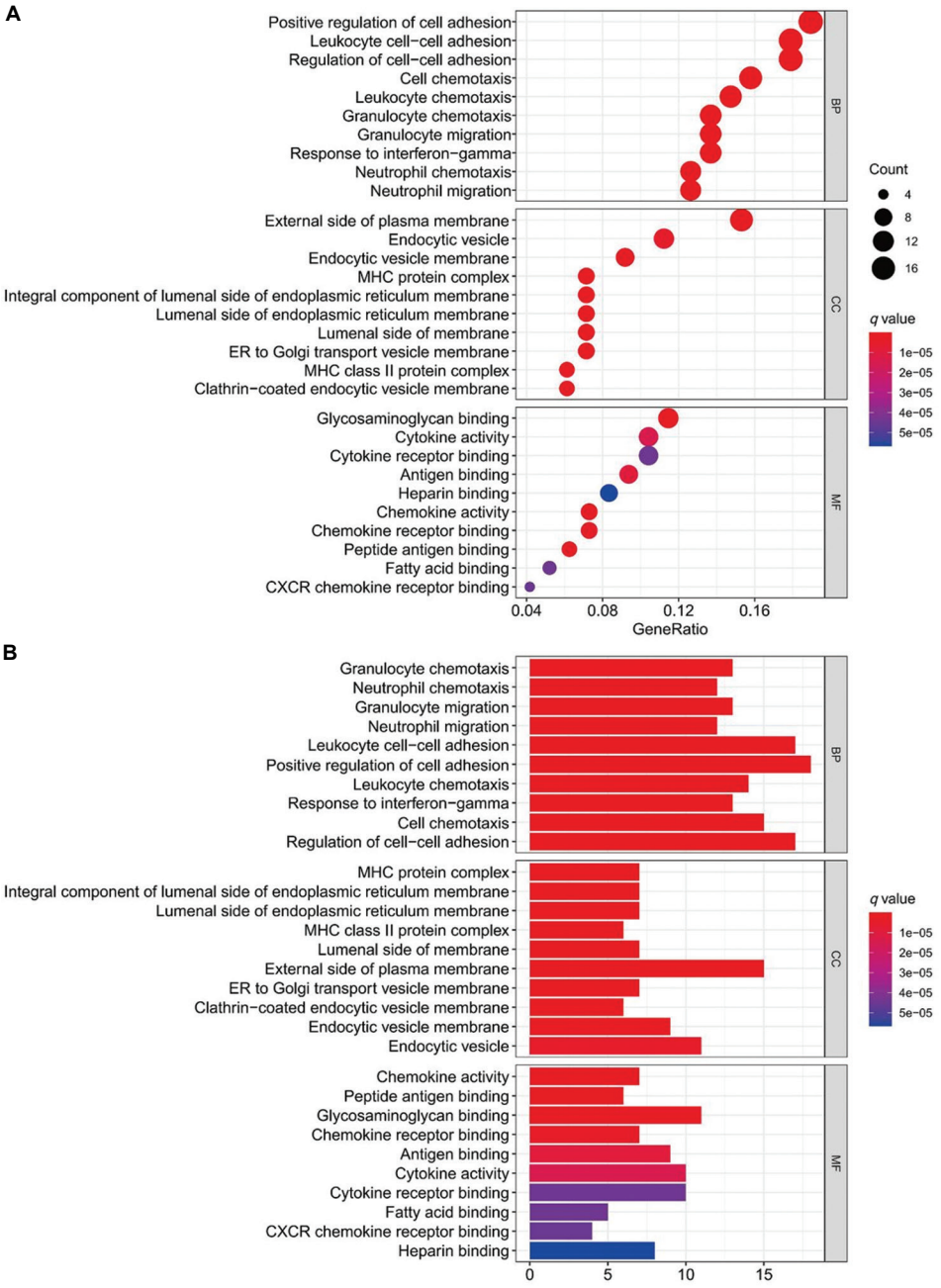


Figure 7. Functional analysis based on The Cancer Genome Atlas cohort's differential genes between the two risk categories
Notes: The larger the bubble, the more genes were enriched, and the deeper the red, the more noticeable the distinctions; *q* value = corrected *P*-value).

motif chemokine ligand 16,[18] especially for brain and lung metastasis.[19] Fifth, DEF6 is a GEF for RAC and CDC42 that is highly expressed in B and T cells. However, in breast tumors, DEF6 regulates the epithelial-to-mesenchymal transformation and movement[20] and the migration, invasion, and production of MMPs. Finally, MATK has an inhibiting effect on the regulation of T-cell proliferation. In breast tumors, MATK inhibits this proliferation by suppressing the activation of ErbB-2/neu-mediated Src family kinases through its SH2 domain to inhibit non-dependent growth and cell invasion.[21,22] As mentioned earlier, *DIRAS3*, *MMP7*, *DEF6*, and *MATK* were down-regulated in BC, indicating that further research may be required to discover how they mediated BC cells, and a joint study of BC and immune pathways may be carried out in the future.

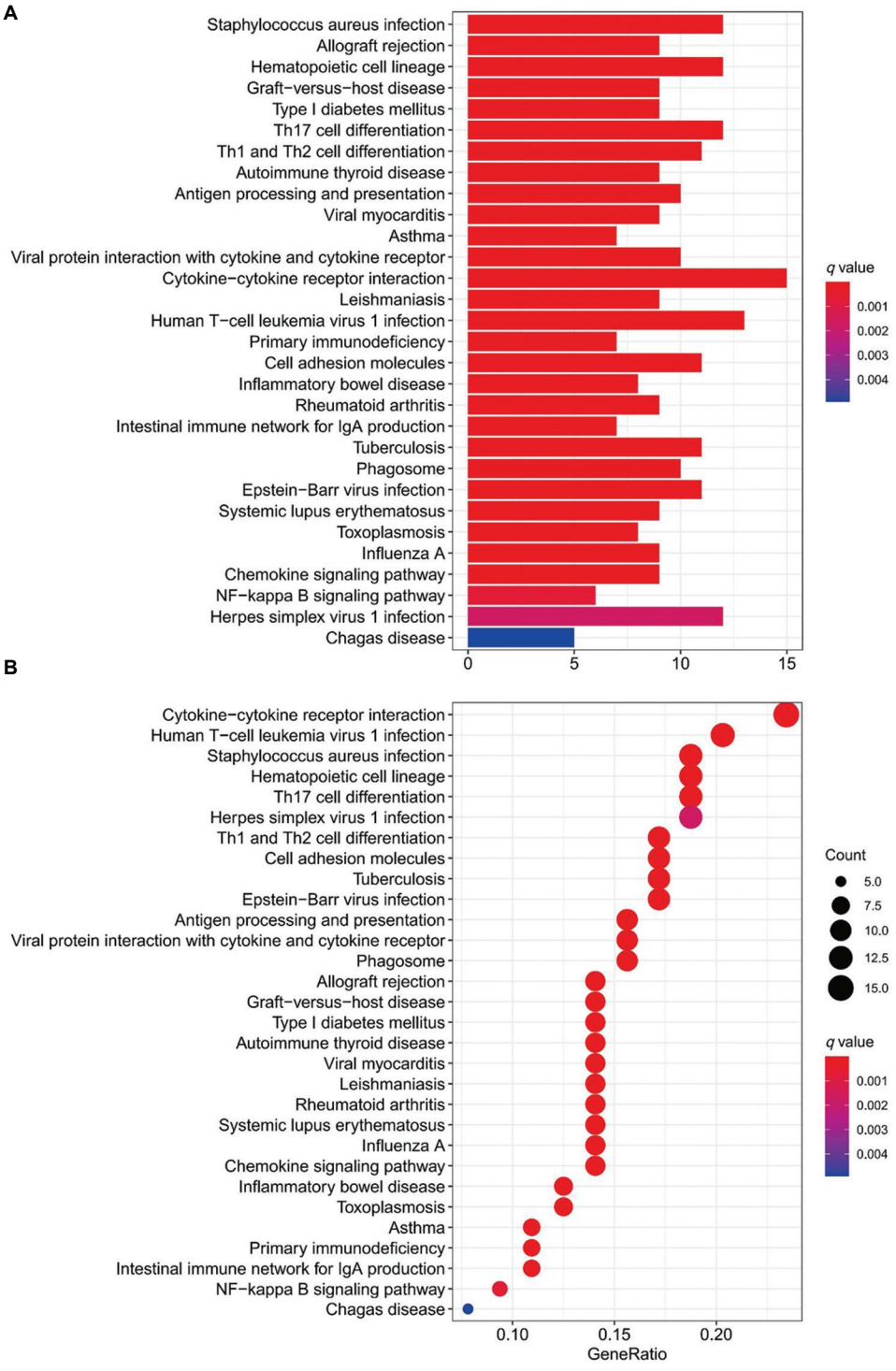


Figure 8. Functional analysis based on The Cancer Genome Atlas cohort's differential genes between the two risk groups
Notes: The larger the bubble, the more genes were enriched, and the deeper the red, the more noticeable the differences; *q* value = adjusted *P*-value).

Except for the association with invasion and metastasis, CACNA1H is closely correlated with both apoptosis and autophagy. Down-regulation of *CACNA1H* on malignant mesothelioma cells reduced *in vitro* epigallocathechin-3-gallate selective cytotoxicity and abated apoptosis and necrosis.[23] However, *CACNA1H* had no significant

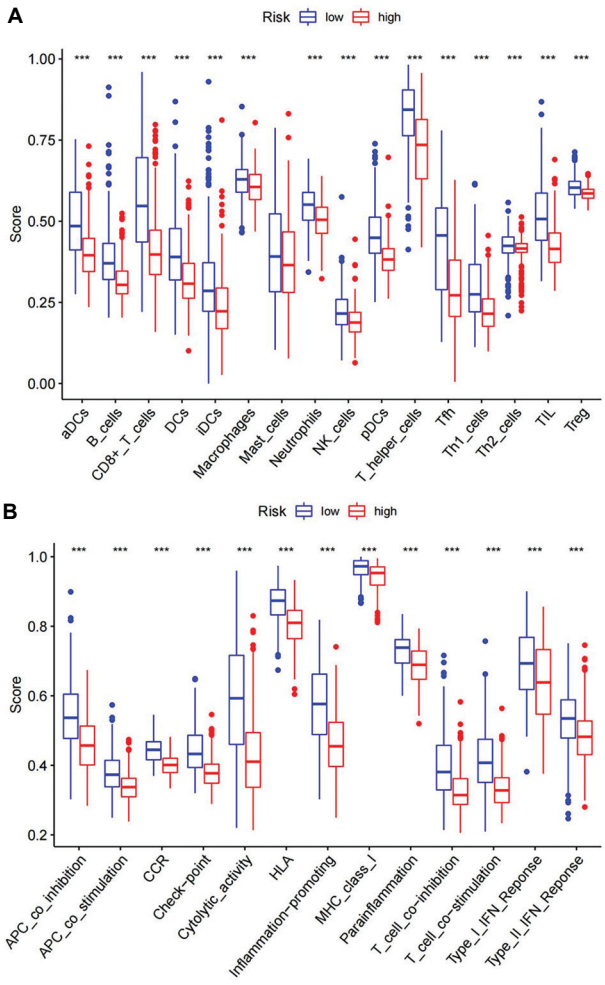


Figure 9. Single-sample gene set enrichment analysis scores for immunological pathways and immune cells compared
Notes: Low-risk group in blue; high-risk group in red; *P*-values: $^{*}P < 0.05$; $^{**}P < 0.01$; $^{***}P < 0.001$.

inhibitory effect on proliferation and apoptosis in MCF-7.[24] Another study showed that expression of *CACNA1H* was closely related to Glut1 and Ki67, the latter possibly associated with autophagy marker LC3.[25]

In addition to being associated with invasion, *MATK* is associated with mitosis and limits the invasion of BC cells by delaying mitosis. Apart from *MATK*, HSPB8 with a conservative alpha-crystallin domain at the C-terminal part of the molecule is also related to mitosis. It enables the cells to cross the G0/G1 phase restriction point to promote the division of BC cells.[26] In this analysis, *MATK* was found to be down-regulated while *HSPB8* was up-regulated. As a consequence, these genes may present novel and distinct prediction targets.

In addition, the cytidine deaminase gene family (*APOBEC3D* and *APOBEC3F*) genes identified in the present study are significantly associated with mitosis.[27] Thus, they may point to additional pathways for BC progression. The down-regulation of *RGS1* may be closely related to DNA methylation-dependent silencing or immune escape. The *RGS1*, a member of the G protein signal transduction family, is an important tumor immune escape site.[28] Due to *RGS1* being down-regulated in this analysis, a joint study of BC and immune pathways may be carried out in the future.

The *PSME2* might be a significant oncogene or tumor suppressor gene for the prevention or early diagnosis of BC. *PSME2*, which plays the role of an oncogene or tumor suppressor gene through multiple pathways in BC, endometrial cancer, and other malignant tumors, is implicated in immunoproteasome assembly and is required for efficient antigen processing. In this study, *PSME2* was down-regulated in BC, indicating that the diagnosis and recurrence of BC may be related to its misregulation.

In the risk model, several genes related to BC have not yet been extensively studied or have unclear pathways, including *PXDNL*, *ARMH1*, and *APOBEC3F*. First, up-regulated *PXDNL*, a member of the peroxidase gene family, has been identified as a potential independent prognostic biomarker for BC, and it appears to be associated with reduced OS and recurrence-free survival rates.[29] Second, *ARMH1*, also known as C1orf228, has been investigated in only three studies, with its relevance primarily noted in oral squamous cell carcinoma. Unfortunately, its pathway in BC remains unclear. Finally, *APOBEC3D* and *APOBEC3F*, which are pseudogenes, have been widely reported, for example, as the genomes of solid tumors, such as BC, cervical cancer, and ovarian cancer.[30-33] Other studies[34] have also identified that *APOBEC3B* was down-regulated in BC tissues. In summary, *PXDNL*, *ARMH1*, *APOBEC3D*, and *APOBEC3F* are promising candidates for further investigation due to their potential applications in BC.

However, contrary to current research, our study discovered that some genes differed in tumor tissue, such as *KLHDC7B*. Kelch domain-containing 7B (KLHDC7B), a protein with 595 amino acid residues, was down-regulated in the tumor tissue in our analysis. Conversely, the up-regulation of *KLHDC7B* expression in BC has been associated with poor prognosis and differentiation grade.[35] As a result of their possible involvement in tumor growth and progression, these findings suggest that *KLHDC7B* could be exploited in tumor diagnosis and as a therapy target.

To sum up (Table 2), *ARMH1*, *APOBEC3D*, *APOBEC3F*, and *PXDNL* are either rarely reported or not previously

Table 2. The pathway of 15 genes (null: The pathway has not been fully elucidated in breast cancer)

Name	Related cancer	Pathway
High-risk genes		
FIBCD1	Breast cancer, gastric cancer, etc.	Inhibit inflammatory mediators and mucinous proteins (GeneCards)
CACNA1H	Breast cancer, prostate cancer, etc.	β-catenin/HMGA2 signaling[13]
HSPB8	Breast cancer, lung cancer, gastric cancer, etc.	Pass the G0/G1 phase restriction point[26]
PXDNL	Breast cancer	Null[29,36,37]
Low-risk genes		
PSME2	Breast cancer, gastric cancer, etc.	Activate proteasomes to generate the antigenic peptides presented by major histocompatibility complex class I molecules[38]
DIRAS3	Breast cancer, ovarian cancer, pancreatic cancer, etc.	Inhibit signaling through PI3 kinase/AKT, JAK/STAT, and RAS/MAPK[16]
RAC2	Breast cancer, pancreatic cancer, etc.	Activated by the combination Gαi-2 and ELMO1/Dock180 complex×[17]
MMP7	Breast cancer, gastric cancer, prostate cancer, colon cancer, etc.	Suppress the recruitment of CD4+/CD8+TILs or the expression of *CXCL16*[18]
MATK	Breast cancer, colon cancer, etc.	Inhibit the activation of Src family kinases[22]
RGS1	Breast cancer, ovarian cancer, gastric cancer, etc.	Suppress CXCR4[39]
KLHDC7B	Breast cancer, bladder cancer, etc.	STAT1-mediated interferon signaling pathway[40]
DEF6	Breast cancer, ovarian cancer, colon cancer, etc.	Suppress E-cadherin expression and the regulation of epithelial-mesenchymal transition transcription factors[20]
ARMH1/APOBEC3D/APOBEC3F	Acute myeloid leukemia, breast cancer, etc.	Null[41]

Abbreviations: *CXCL16*: C-X-C motif chemokine ligand 16; TILs: Tumor-infiltrating lymphocytes; FIBCD1: Fibrinogen C domain-containing 1; *CACNA1H*: Calcium voltage-gated channel subunit alpha1 H; *HSPB8*: Heat shock protein family B (small) member 8; *PXDNL*: Peroxidasin-like; *PSME2*: Proteasome activator subunit 2; *ARMH1*: Armadillo-like helical domain-containing 1; DIRAS3: DIRAS family GTPase 3; *MMP7*: Matrix metallopeptidase 7; *MATK*: Megakaryocyte-associated tyrosine kinase; *RGS1*: Regulator of G protein signaling 1.

studied in BC literature. Thus, these four genes can be used as target genes for further BC research. In addition, we found that *CACNA1H*, *RAC2*, *DIRAS3*, and *DEF6* are intimately associated with the invasion and metastasis of BC cells, so new ways might be found to prevent and treat BC or improve its prognosis by promoting the combined up-regulation or down-regulation of these four genes. In addition, the down-regulation of *DEF6* is closely related to MMPs, suggesting that these two genes might be potential indicators for further prognosis of BC.

The innovation of this study lies in the construction of a highly reliable prognosis model based on 15 risk genes. We identified specific links between different genes, which promoted multidisciplinary analysis and provided personalized prevention and treatment for different patients with BC. However, the limitation of this study is that the *P*-value of the prognosis model is 0.01, and the genes selected are large, which is not conducive to analysis. Reducing the *P*-value could potentially narrow down the number of prognostic genes and refine the model.

As shown in Table 2, we performed qPCR and western blotting to investigate the expression level of pyroptosis-related genes in BC based on gene and protein levels. As shown in Figure 10, the qPCR results are generally consistent with those of Western blotting. In MDA-MB-231 cells and MDA-MB-468 cells, the expressions of *APOBEC3D* and *APOBEC3F* were much higher than in BT549 and MCF7. It is worth noting that the proteins APOBEC3D and APOBEC3F were used with the same antibody in western blotting. Moreover, a low expression of *APOBEC3D* in MCF7 was also reported by Chen *et al.*[42] In addition, the expressions of *PXDNL* and *ARMH1* were significantly higher in BC cells, indicating that they may be used as therapeutic targets in BC.[43,44]

Similarly, there are several limitations to this study. Primarily, it relies on bioinformatics analysis using data from public databases, meaning that all predictions require further experimental validation.[45] While we conducted some preliminary verification, such as *in vitro* verification of gene expression and protein levels in BC cell lines,

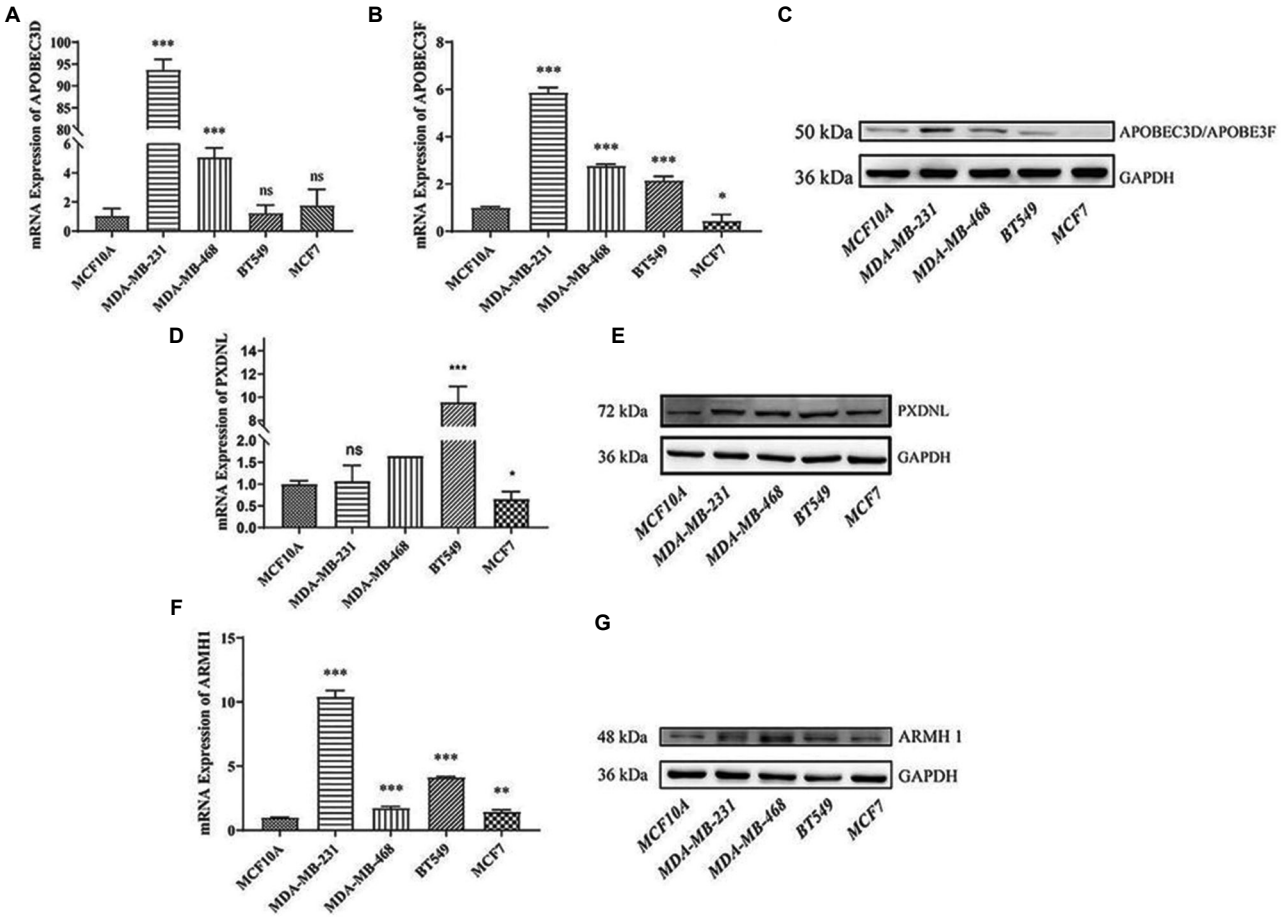


Figure 10. (A-C) Expression of prognostic genes in breast cancer (BC). In MDA-MB-231 cells and MDA-MB-468 cells, the expressions of *APOBEC3D* and A*POBEC3F* were much higher than in BT549 and MCF7. Notably, the same antibody was used for detecting both proteins APOBEC3D and APOBEC3F in western blotting. (D-G) In addition, the expressions of *PXDNL* and *ARMH1* were significantly higher in BC cells.
Notes: *P*-values: ns = not significant; **P* < 0.05; ***P* < 0.01; ****P* < 0.001.

additional research is needed to address the remaining questions and confirm these findings.

5. Conclusion

We identified four high-risk genes – *FIBCD1*, *CACNA1H*, *HSPB8*, and *PXDNL* – that are involved in BC pyroptosis. Notably, the expression of *PXDNL* was significantly elevated in BC cells *in vitro*, suggesting that *PXDNL* could serve as a new target for early diagnosis and prognosis in BC.

Acknowledgments

None.

Funding

This work was supported by the Administration of Traditional Chinese Medicine of Guangdong Province (No. 20221218).

Conflict of interest

The authors declare that the research was conducted in the absence of any commercial or financial relationships that could be construed as a potential conflicts of interest.

Author contributions

Conceptualization: Shanshan Wang, Dashuang Yang, Jiaqian Mo
Formal analysis: Moxian Chen
Investigation: Shanshan Wang, Dashuang Yang, Jiaqian Mo
Methodology: Shanshan Wang, Dashuang Yang, Jiaqian Mo
Writing-original draft: Shanshan Wang, Dashuang Yang, Jiaqian Mo
Writing-review & editing: Rongxin Zhang

Ethics approval and consent to participate

All BC clinical data were downloaded from the TCGA database. The data provided by the database are ethically

approved and compliant with relevant research ethics standards.

Consent for publication

Not applicable.

Availability of data

All data and materials supporting the findings of this work are available from the corresponding author upon reasonable request.

References

1. Nolan E, Lindeman GJ, Visvader JE. Deciphering breast cancer: From biology to the clinic. *Cell*. 2023;186(8):1708-1728.

   doi: 10.1016/j.cell.2023.01.040

2. Ye F, Dewanjee S, Li Y, *et al*. Advancements in clinical aspects of targeted therapy and immunotherapy in breast cancer. *Mol Cancer*. 2023;22(1):105.

   doi: 10.1186/s12943-023-01805-y

3. *Breast Cancer*. Available from: https://www.who.int/news-room/fact-sheets/detail/breast-cancer [Last accessed on 2024 Feb 21].

4. GBD 2019 Diseases and Injuries Collaborators. Global burden of 369 diseases and injuries in 204 countries and territories, 1990-2019: A systematic analysis for the Global Burden of Disease Study 2019. *Lancet*. 2020;396(10258):1204-1222.

   doi: 10.1016/S0140-6736(20)30925-9

5. Zhou Z, He H, Wang K, *et al*. Granzyme A from cytotoxic lymphocytes cleaves GSDMB to trigger pyroptosis in target cells. *Science*. 2020;368(6494):eaaz7548.

   doi: 10.1126/science.aaz7548

6. Xing Y, Zhang F, Ji P, *et al*. Efficient delivery of GSDMD-N mRNA by engineered extracellular vesicles induces pyroptosis for enhanced immunotherapy. *Small*. 2023;19(20):2204031.

   doi: 10.1002/smll.202204031

7. Newton K, Strasser A, Kayagaki N, Dixit VM. Cell death. *Cell*. 2024;187(2):235-256.

   doi: 10.1016/j.cell.2023.11.044

8. Guo X, Bian Y, Zhang Y, Yu H, Yu X. Research progress of mechanism of non-coding RNA-regulated pyroptosis in atherosclerosis. *Pract J Card Cereb Pneumal Vasc Dis*. 2021;29(12):136-140.

9. Tsuchiya K. Inflammasome-associated cell death: Pyroptosis, apoptosis, and physiological implications. *Microbiol Immunol*. 2020;64(4):252-269.

   doi: 10.1111/1348-0421.12771

10. Chen C, Ye Q, Wang L, *et al*. Targeting pyroptosis in breast cancer: Biological functions and therapeutic potentials on It. *Cell Death Discov*. 2023;9:75.

    doi: 10.1038/s41420-023-01370-9

11. Wang Y, Sun M, Liu J, *et al*. FIBCD1 overexpression predicts poor prognosis in patients with hepatocellular carcinoma. *Oncol Lett*. 2020;19(1):795-804.

    doi: 10.3892/ol.2019.11183

12. Vishnubalaji R, Alajez NM. Epigenetic regulation of triple negative breast cancer (TNBC) by TGF-β signaling. *Sci Rep*. 2021;11(1):15410.

    doi: 10.1038/s41598-021-94514-9

13. Li S, Hao M, Li B, *et al*. CACNA1H downregulation induces skeletal muscle atrophy involving endoplasmic reticulum stress activation and autophagy flux blockade. *Cell Death Dis*. 2020;11(4):279.

    doi: 10.1038/s41419-020-2484-2

14. Sharma S, Wu SY, Jimenez H, *et al*. Ca2+ and CACNA1H mediate targeted suppression of breast cancer brain metastasis by AM RF EMF. *EBioMedicine*. 2019;44:194-208.

    doi: 10.1016/j.ebiom.2019.05.038

15. Nanba K, Blinder AR, Rege J, *et al*. Somatic CACNA1H mutation as a cause of aldosterone-producing adenoma. *Hypertens Dallas Tex 1979*. 2020;75(3):645-649.

    doi: 10.1161/HYPERTENSIONAHA.119.14349

16. Bildik G, Liang X, Sutton MN, Bast RC, Lu Z. DIRAS3: An imprinted tumor suppressor gene that regulates RAS and PI3K-driven cancer growth, motility, autophagy, and tumor dormancy. *Mol Cancer Ther*. 2022;21(1):25-37.

    doi: 10.1158/1535-7163.MCT-21-0331

17. Li H, Yang L, Fu H, *et al*. Association between Gαi2 and ELMO1/Dock180 connects chemokine signalling with Rac activation and metastasis. *Nat Commun*. 2013;4:1706.

    doi: 10.1038/ncomms2680

18. Yuan JQ, Zhang KJ, Wang SM, Guo L. YAP1/MMP7/CXCL16 axis affects efficacy of neoadjuvant chemotherapy via tumor environment immunosuppression in triple-negative breast cancer. *Gland Surg*. 2021;10(9):2799-2814.

    doi: 10.21037/gs-21-612

19. Sizemore ST, Sizemore GM, Booth CN, *et al*. Hypomethylation of the MMP7 promoter and increased expression of MMP7 distinguishes the basal-like breast cancer subtype from other triple-negative tumors. *Breast Cancer Res Treat*. 2014;146(1):25-40.

    doi: 10.1007/s10549-014-2989-4

20. Zhang Z, Yang M, Chen R, *et al*. IBP regulates epithelial-to-mesenchymal transition and the motility of breast cancer cells via Rac1, RhoA and Cdc42 signaling pathways.

Oncogene. 2014;33(26):3374-3382.

doi: 10.1038/onc.2013.337

21. Bougeret C, Jiang S, Keydar I, Avraham H. Functional analysis of Csk and CHK kinases in breast cancer cells. *J Biol Chem*. 2001;276(36):33711-33720.

doi: 10.1074/jbc.M104209200

22. Kim S, Zagozdzon R, Meisler A, *et al*. Csk homologous kinase (CHK) and ErbB-2 interactions are directly coupled with CHK negative growth regulatory function in breast cancer. *J Biol Chem*. 2002;277(39):36465-36470.

doi: 10.1074/jbc.M206018200

23. Ranzato E, Martinotti S, Magnelli V, *et al*. Epigallocatechin-3-gallate induces mesothelioma cell death via H2O2-dependent T-type Ca2+ channel opening. *J Cell Mol Med*. 2012;16(11):2667-2678.

doi: 10.1111/j.1582-4934.2012.01584.x

24. Ohkubo T, Yamazaki J. T-type voltage-activated calcium channel Cav3.1, but not Cav3.2, is involved in the inhibition of proliferation and apoptosis in MCF-7 human breast cancer cells. *Int J Oncol*. 2012;41(1):267-275.

doi: 10.3892/ijo.2012.1422

25. Maiques O, Macià A, Moreno S, *et al*. Immunohistochemical analysis of T-type calcium channels in acquired melanocytic naevi and melanoma. *Br J Dermatol*. 2017;176(5): 1247-1258.

doi: 10.1111/bjd.15121

26. Cristofani R, Piccolella M, Crippa V, *et al*. The role of HSPB8, a component of the chaperone-assisted selective autophagy machinery, in cancer. *Cells*. 2021;10(2):335.

doi: 10.3390/cells10020335

27. Lackey L, Law EK, Brown WL, Harris RS. Subcellular localization of the APOBEC3 proteins during mitosis and implications for genomic DNA deamination. *Cell Cycle Georget Tex*. 2013;12(5):762-772.

doi: 10.4161/cc.23713

28. Huang D, Chen X, Zeng X, *et al*. Targeting regulator of G protein signaling 1 in tumor-specific T cells enhances their trafficking to breast cancer. *Nat Immunol*. 2021;22(7): 865-879.

doi: 10.1038/s41590-021-00939-9

29. Li Y, Jiao Y, Luo Z, Li Y, Liu Y. High peroxidasin-like expression is a potential and independent prognostic biomarker in breast cancer. *Medicine* (*Baltimore*). 2019;98(44):e17703.

doi: 10.1097/MD.0000000000017703

30. Revathidevi S, Murugan AK, Nakaoka H, Inoue I, Munirajan AK. APOBEC: A molecular driver in cervical cancer pathogenesis. *Cancer Lett*. 2021;496:104-116.

doi: 10.1016/j.canlet.2020.10.004

31. Shen B, Chapman JH, Custance MF, Tricola GM, Jones CE, Furano AV. Perturbation of base excision repair sensitizes breast cancer cells to APOBEC3 deaminase-mediated mutations. *Elife*. 2020;9:e51605.

doi: 10.7554/eLife.51605

32. Smith NJ, Fenton TR. The APOBEC3 genes and their role in cancer: Insights from human papillomavirus. *J Mol Endocrinol*. 2019;62(4):R269-R287.

doi: 10.1530/JME-19-0011

33. Law EK, Levin-Klein R, Jarvis MC, *et al*. APOBEC3A catalyzes mutation and drives carcinogenesis *in vivo*. *J Exp Med*. 2020;217(12):e20200261.

doi: 10.1084/jem.20200261

34. Burns MB, Lackey L, Carpenter MA, *et al*. APOBEC3B is an enzymatic source of mutation in breast cancer. *Nature*. 2013;494(7437):366-370.

doi: 10.1038/nature11881

35. Martín-Pardillos A, Cajal SRY. Characterization of Kelch domain-containing protein 7B in breast tumours and breast cancer cell lines. *Oncol Lett*. 2019;18(3):2853-2860.

doi: 10.3892/ol.2019.10672

36. Zhao H, Yin X, Wang L, *et al*. Identifying tumour microenvironment-related signature that correlates with prognosis and immunotherapy response in breast cancer. *Sci Data*. 2023;10(1):119.

doi: 10.1038/s41597-023-02032-2

37. Tian W, Luo Y, Tang Y, *et al*. Novel implication of the basement membrane for breast cancer outcome and immune infiltration. Int J Biol Sci. 2023;19:1645-1663.

doi: 10.7150/ijbs.81939

38. Qi A, Ju M, Liu Y, *et al*. Development of a novel prognostic signature based on antigen processing and presentation in patients with breast cancer. *Pathol Oncol Res*. 2021;27:600727.

doi: 10.3389/pore.2021.600727

39. Bjarnadottir O, Kimbung S, Johansson I, *et al*. Global transcriptional changes following statin treatment in breast cancer. *Clin Cancer Res*. 2015;21(15):3402-3411.

doi: 10.1158/1078-0432.CCR-14-1403

40. Jeong G, Bae H, Jeong D, *et al*. A Kelch domain-containing KLHDC7B and a long non-coding RNA ST8SIA6-AS1 act oppositely on breast cancer cell proliferation via the interferon signaling pathway. *Sci Rep.* 2018;8(1):12922.

doi: 10.1038/s41598-018-31306-8

41. Mumme H, Thomas BE, Bhasin SS, *et al*. Single-cell analysis reveals altered tumor microenvironments of relapse- and remission-associated pediatric acute myeloid leukemia. *Nat Commun*. 2023;14:6209.

doi: 10.1038/s41467-023-41994-043

42. Chen Q, Jun H, Yang C, Yang F, Xu Y. The pyroptosis-related risk genes APOBEC3D, TNFRSF14, and RAC2 were used to evaluate prognosis and as tumor suppressor genes in breast cancer. *J Oncol*. 2022;2022:3625790

    doi: 10.1155/2022/3625790

43. Jia ZC, Yang X, Wu YK, *et al*. The art of finding the right drug target: Emerging methods and strategies. *Pharmacol Rev.* 2024;76:896-914.

    doi: 10.1124/pharmrev.123.00102844

44. Yang X, Li M, Jia ZC, *et al*. Unraveling the secrets: Evolution of resistance mediated by membrane proteins. *Drug Resist Updat.* 2024;77:101140.

    doi: 10.1016/j.drup.2024.10114045

45. Liu H, Chen X, Jia Y, *et al*. Facing inevitable PARPis resistance: Mechanisms and therapeutic strategies for breast cancer treatment. *Interdiscipl Med*. 2023;1:e20220013.

    doi: 10.1002/INMD.20220013